Journal of Chromatography, 185 (1979) 79–95

CHROM. 12,328

EXTRA-COLUMN EFFECTS IN HIGH-PERFORMANCE LIQUID CHROMATOGRAPHY

I. THEORETICAL STUDY OF THE INJECTION PROBLEM

HENRI COLIN, MICHEL MARTIN and GEORGES GUIOCHON

Laboratoire de Chimie Analytique Physique, École Polytechnique, Route de Saclay, 91128 Palaiseau-Cedex (France)

SUMMARY

The effect of the injection process on the column efficiency depends on the injection time, the injection volume and the technique of sampling (syringe on-line or stop-flow injection through a septum-type injector port or valve injection in either the normal or the split mode).

The injection process can be described by a contribution to the plate height that is proportional to the square of the length of the solute zone at the column inlet (Δx) and inversely proportional to the square of the column length and to a constant describing the concentration profile in the solute zone.

A simple model based on the combined effect of solute displacement due to the injection flow and to the mobile phase flow makes possible the calculation of Δx. The effects of injection time and volume are complex and depend on the sampling system and on geometrical parameters such as the column internal cross-sectional area, the sampling canal internal and external cross-sectional areas and two coefficients related to the flow pattern at the column inlet. In some conditions, the model proposed predicts, in agreement with experimental results, a non-linear dependence of the plate height on the square of the injection volume.

Finally, the influence of particle size on the extra-column effect due to injection depends closely on the experimental conditions: the results are different when the column is operated at maximal efficiency and when we want to achieve a given number of theoretical plates in a given time. In some instances the injection effect is independent on the particle size and in others it is inversely proportional to d_p^4.

INTRODUCTION

The use of microparticulate packings in high-performance liquid chromatography (HPLC) makes it possible to prepare efficient columns, yielding at least 50,000 theoretical plates per metre, in reasonably short times. However taking full advantage of such materials is possible only if on the one hand efficient packing pro-

cedures are available, and on the other the extra-column effects are controlled so as not to increase appreciably the band width or to distort the peak shape.

Much work has been devoted to the art of column packing (*e.g.*, refs. 1–3). It does not seem that there is a universally accepted procedure and several different techniques yield column with a minimum reduced plate height in the range 2–4. It is often reported that good results are obtained with silica gel using a slurry of the particles in carbon tetrachloride. With the appropriate modification, this method is also very convenient for packing of reversed-phase columns.

Extra-column effects occur both before the column inlet (injection) and after the column outlet (detection). The problems associated with detection will be considered in a following paper[4]. The major role of injection in liquid chromatography has long been recognized. In 1969, Smuts *et al.*[5] noted that "In liquid chromatography, there is reason to believe that the inlet system can ultimately be the limiting factor". More recently, Kirkland *et al.*[6] wrote that "...sampling can be a major cause of band broadening in HPLC because of extra-column effects", and Simpson[7] noted that "The manner in which the sample is introduced to the column in liquid chromatography is one of the most critical steps in obtaining a good separation". This problem has not been given a completely satisfactory solution yet and few detailed surveys of it have been undertaken in the past.

It is often said that the smaller the particle size or the more efficient the column, the bigger are the extra-column effects. In fact, the relative contribution of the injection process to band spreading depends on the solute retention volume and retention time and on the extent of band spreading in the column itself. For a given injection method, the smaller these parameters, the larger is the relative contribution of extra-column effects. The development of 5-μm particles has generally been accompanied by a decrease in column length and hence in retention time and volume. This explains why the extra-column effects are considered to be more important when using small particles. In fact, the efficiency, the analysis time and the flow-rate are the key parameters.

This paper is devoted to a theoretical approach in the injection process. The experimental results are given in Part II[8].

THEORETICAL

Estimation of column efficiency

The most convenient way of comparing various injection systems is to measure the variance of the signal obtained when injecting a test solute. Most often the injection process can be described by Gaussian and exponential operators acting on the solute distribution inlet function[9]. Consequently, even if the solute dispersion in the column is Gaussian, the peak shape at the outlet of the column is not necessarily Gaussian. This means that when trying to evaluate column performance by measurement of peak symmetry, as has been suggested[6,10], attention must be paid to the quality of the injection system, which must be virtually perfect as pointed out by Kirkland *et al.*[6].

There are several methods for measuring column efficiencies from peak profiles[11]:

(1) without geometrical construction, *ca.* peak width at a given fraction of the peak height (usually 0.5 or 0.606);

(2) with geometrical construction, baseline width determined by inflexion tangents;

(3) with an integrator, ratio of peak area to peak height;

(4) with a computer, normalized second moment.

Only the last method gives the exact efficiency, but as long as the signal is Gaussian, all of these procedures are equivalent. However, as demonstrated by Kirkland *et al.*[6], the first method (peak width at half-height) gives the least exact estimate of the signal variance when the distribution is not Gaussian. In that case, measurements (1) and (2) overestimate the actual efficiency[6,11]. The simplified plate count methods are valid only if the peak skew is less than 0.7. This is unfortunate, as most often only methods (1) and (2) can be used by chromatographers. From a theoretical point of view the measure of the second moment is the only correct method. From a practical point of view, however, it is questionable whether the exact measure of column efficiency or the simplified one using (1) and (2) is the more significant.

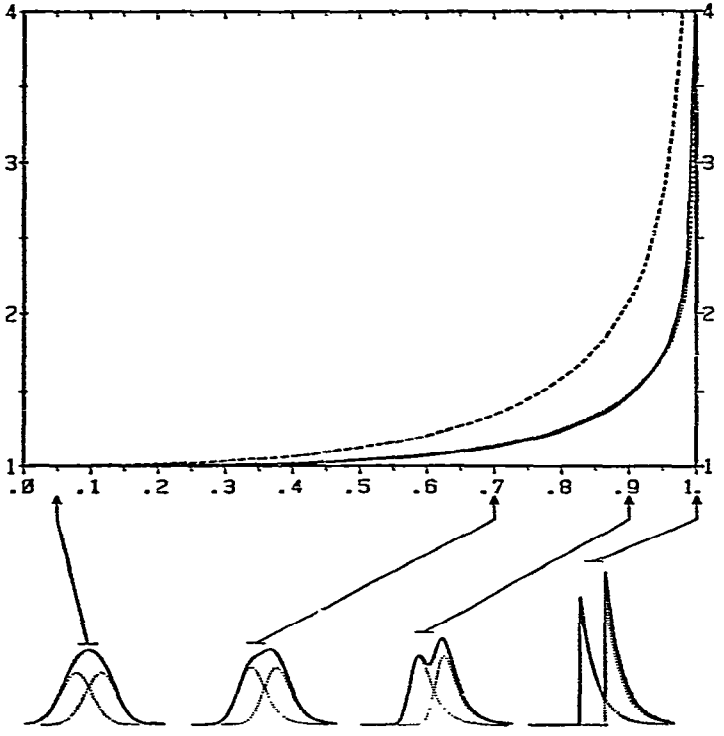

Fig. 1. Variation of the relative resolution and peak asymmetry *versus* the τ/σ ratio for exponentially modified Gaussian peaks. τ is the exponential time constant, σ the total standard deviation of the peak, kept constant. - - - - - -, Peak asymmetry (measured at 10% of the peak height); · · · · ·, ratio of the resolution calculated from the peak width at the baseline over the standard deviation (σ) based resolution; ——, ratio of the resolution calculated from the peak width at half-height over the standard deviation (σ) based resolution. The standard deviation based resolution is kept constant at 0.4. The chromatograms of the two equal peaks are shown for τ/σ ratios of 0.05, 0.7, 0.9 and 1.0.

This is shown in Fig. 1, which gives plots for two exponentially modified Gaussian peaks of the resolution calculated under various conditions versus the τ/σ ratio. τ and σ^2 are the time constant of the exponential and the total variance of the peak which is kept constant, respectively. Under this condition the resolution ($R_s = \Delta t_R/4\sigma$) based on the peak variance also remains constant. For this reason, the two resolution curves shown in Fig. 1 (resolution calculated from either half-height or baseline peak width) are expressed relative to this variance (second moment) based resolution. We have also given in Fig. 1 the variation of the asymmetry (measured at 10% of the peak height) with τ/σ. In addition, for some particular values of τ/σ the corresponding chromatograms are given. The variance-based resolution is 0.4 and the two peaks are not resolved when they are Gaussian. It must be pointed out that the column contribution to bandbroadening on Fig. 1 decreases as τ/σ increases in order to keep the total variance constant. The dotted lines on the chromatograms correspond to the individual peaks. The increase in peak height with τ/σ is due the fact that the peak surface area was kept constant. It is certain that the analyst will prefer the separation corresponding to a high value of τ/σ (0.9 or 1.0) rather than a low value. Although the real plate number (based on variance or second moment) is the same for all peaks, it is clear that the measurement of column efficiency from the peak width at half-height (or baseline) gives a better estimation of the ability of the column to separate close asymmetrical peaks. We should point out, however, that in most practical cases the three values of the resolution are very close.

Efficiency of injection

The injection process is characterized by three parameters: the injection volume, $V_{inj.}$, the injection time, $t_{inj.}$, and the design of the system, which is related to the flow pattern at the column inlet and to the quality of the injector. This is described by the constant K in the equations below.

The injection process therefore depends on the injector and the connector devices. According to the type of injector selected, $V_{inj.}$ and $t_{inj.}$ may or may not be independent variables. The effects of $V_{inj.}$ and $t_{inj.}$ have been studied by several workers[6,9,12–15]. The combination of the two effects needs a careful analysis, however.

The variance of the solute band at the outlet of the column ($\sigma^2_{out.}$) is the sum of the variance of the chromatographic process itself ($\sigma^2_{col.}$) and the variance of the injection process ($\sigma^2_{inj.}$). If these variances are calculated on a time basis, then

$$\sigma^2_{t,out.} = \sigma^2_{t,col.} + \sigma^2_{t,inj.} \tag{1}$$

Eqn. 1 can be rewritten using the retention time, t_R, and the number of theoretical plates, defined as follows:

$$\sigma^2_{t,out.} = \frac{t_R^2}{N_{out.}}; \sigma^2_{t,col.} = \frac{t_R^2}{N_{col.}}; \sigma^2_{t,inj.} = \frac{t_R^2}{N_{inj.}} \tag{2}$$

Combination of eqns. 1 and 2 gives

$$\frac{1}{N_{out.}} = \frac{1}{N_{col.}} + \frac{1}{N_{inj.}} \tag{3}$$

$N_{out.}$ is the number of theoretical plates at the outlet of the column, $N_{col.}$ is the contribution of the column and $N_{inj.}$ is the contribution of the injection process. In fact, $N_{out.}$ is also the number of theoretical plates measured on the chromatogram if $\sigma^2_{t,col.}$ is the sum of the variances of the column and of the extra-column effects, except the injection accounted for in eqn. 1 by $\sigma^2_{t,inj.}$. Eqn. 3 is equivalent to the more conventional expression relating the corresponding plate height contributions (see eqn. 12).

Eqn. 3 indicates that if the injection is perfect ($N_{inj.} \rightarrow \infty$) then $N_{out.} = N_{col.}$. On the other hand, if the injection is particularly bad ($N_{inj.} \rightarrow 0$) then $N_{out.} = N_{inj.}$. The quality of the injection can therefore be described by a number of theoretical plates, similarly to the column quality. We should point out at this stage, however, that $N_{inj.}$ will depend not only on the injector but also on the column used. In order to calculate $N_{inj.}$, it is necessary to evaluate $\sigma^2_{t,inj.}$.

The injection process can be characterized by the length, Δx, of the band of solute and by the solute concentration profile at the column inlet. The corresponding variance (length basis) is therefore

$$\sigma^2_{x,inj.} = \frac{\Delta x^2}{K^2} \tag{4}$$

The value of the constant K is related to the concentration profile and has been evaluated for various injection functions by Sternberg[9]. For a rectangular profile, $K^2 = 12$.

Eqn. 4 can also be written on a time basis:

$$\sigma^2_{t,inj.} = \sigma^2_{x,inj.}/v^2 = \frac{\Delta x^2}{K^2 v^2} \tag{5}$$

where v is the velocity of the solute zone, and is related to the mobile phase velocity in the column, u, and to the capacity factor of the column, k', according to the equation

$$v = u/(1 + k') = L/t_R \tag{6}$$

Combination of eqns. 2–6 permits the derivation of

$$N_{inj.} = \frac{K^2 L^2}{\Delta x^2} \tag{7}$$

It appears that $N_{inj.}$ is proportional to L^2, as Δx and K are independent of L, whereas $N_{col.}$ ($= L/H$) is proportional to L. Eqns. 3 and 7 show that for very long columns, $N_{out.}$ is proportional to L, whereas for very short columns it is proportional to L^2, which shows that the shorter the column, the more critical the injection process. The variation of $N_{out.}$ with column length is shown in Fig. 2. The intercept of the asymptote with the L axis is $L_{lim.}$, given by:

$$L_{lim.} = \frac{\Delta x^2}{K^2 H} \tag{8}$$

where H is the column HETP ($L/N_{col.}$).

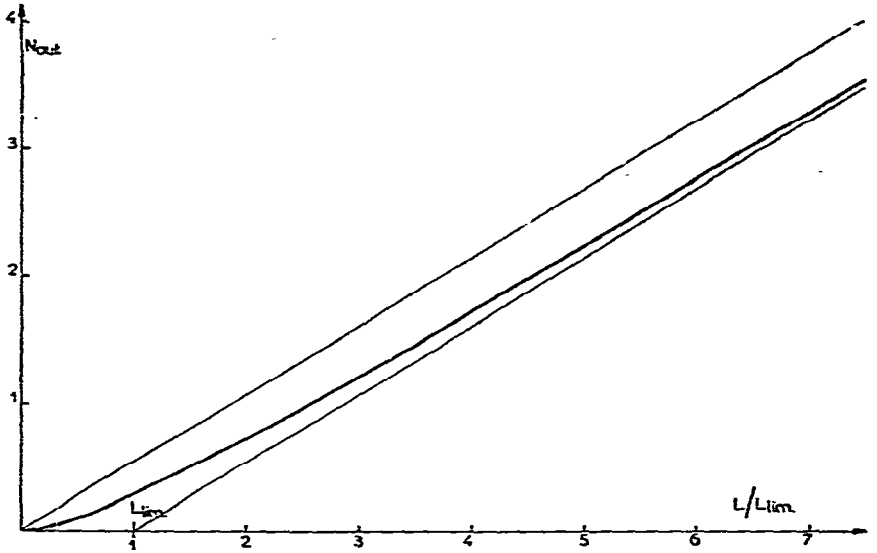

Fig. 2. Variation of $N_{out.}$ (arbitrary units) with $L/L_{lim.}$ (see text). The straight line passing through the origin represents $N_{col.}$, and the other straight line represents the plate number as calculated from eqn. 11.

The loss of efficiency due to the injection process can easily be evaluated from eqns. 3 and 7:

$$N_{col.} - N_{out.} = \frac{L}{H} \cdot \frac{1}{1 + \frac{K^2HL}{\Delta x^2}} \tag{9}$$

For sufficiently long columns, $(K^2HL/\Delta x^2) \gg 1$ and eqn. 9 becomes

$$N_{col.} - N_{out.} = \frac{\Delta x^2}{K^2H^2} \tag{10}$$

The assumption made above is equivalent to $N_{inj.} \gg N_{col.}$ or $\sigma^2_{inj.} \ll \sigma^2_{col.}$. Combination of eqns. 8 and 10 gives

$$N_{out.} = \frac{L - L_{lim.}}{H} \tag{11}$$

Finally, the injection process is equivalent to a reduction in the column length by an amount equal to $L_{lim.}$. This is not valid when the column length is comparable to $L_{lim.}$.

It is also possible to describe the contribution of the injection in terms of reduced plate height (h). If $h_{out.}$ and $h_{col.}$ are the reduced plate height at the column outlet and the column contribution to $h_{out.}$, respectively, then

$$h_{out.} = h_{col.} + \Delta h; \qquad \Delta h = \frac{\Delta x^2}{K^2Ld_p} \tag{12}$$

where d_p is the particle size.

Consider, for instance, a 10-μl injection into a 4-mm I.D. column packed with 5-μm particles and operated at the minimum of the plate height curve ($h_{col.} = 2$); the minimum value of Δx is about 0.8 mm (as shown later) for a slightly retained solute ($k' = 0.33$). We can then calculate from eqns. 8 and 10 that $N_{col.} - N_{out.} = 533$ and $L_{llm.} = 5.3$ mm. For a 20-cm long column the reduced plate height contribution is 0.05, which is almost negligible, and $N_{inj.}$ is 750,000.

The injection model

It is impossible in the general case to give a rigorous mathematical treatment of the contribution of the injection process to the peak variance at the column outlet, because it is very difficult to calculate the concentration profile at column inlet (injection profile or injection function). Indeed, it is related not only to the behaviour of the injection device, but also to the flow pattern at the column inlet, which may change during the injection process. Thus, Δx depends on the injector and on the column parameters (cross-section S_c, permeability K^0, etc). We shall discuss this approach in some simple cases.

The injection contribution to the solute band broadening is due to the finite value of the solute zone width at the column inlet, Δx (eqn. 4). Δx reflects the axial displacement during the injection time of the first injected molecules relative to the position of the last injected molecules.

This displacement results firstly from the sample injection flow in the injection tube (or syringe needle), and secondly from the flow of mobile phase generated by the pumping system around this tube (external flow) which carries the sample away.

These two flows combine to displace the sample. Then the contributions of these two processes to the band-width, Δx_1 and Δx_2, respectively, are not independent and must be added to give Δx:

$$\Delta x = \Delta x_1 + \Delta x_2 \tag{13}$$

with

$$\Delta x_1 = u'_{inj.} t_{inj.} \text{ and } \Delta x_2 = u'_{ext.} t_{inj.} \tag{14}$$

where $u'_{inj.}$ and $u'_{ext.}$ are the linear velocities corresponding, respectively, to the injection flow and external flow described above, averaged over the corresponding flow cross-sections.

At this point it is necessary to choose a model in order to obtain a clearer picture of Δx. We shall express Δx as the length occupied by the solute just after the injection into the packing.

In their discussion, Scott[16] and Snyder[17] agreed that, because of retention, there is a contraction effect of the volume in which the solute is distributed as it enters the packing. We can point out that the time necessary for sorption to take place is, at least for $k' > 1$, of the same order of magnitude as the time needed for diffusion across one particle diameter (d_p), that is, d_p/D_m. It is about 10 msec for typical LC conditions. This time is usually at least one or two orders of magnitude smaller than the injection time. Similarly, in addition to this contraction effect due to retention, there is a dilatation effect, due to the presence of the stationary phase

in the column. This effect is related to the total porosity of the column, ε_T.

On the other hand, the overloading of the first part of the column is kept as small as possible while injecting very diluted samples. Under these conditions, $u'_{inj.}$ is given by

$$u'_{inj.} = \frac{F_{inj.}}{S_{inj.}(1 + k')\varepsilon_T} \cdot \alpha \tag{15}$$

where $F_{inj.}$ is the injection flow-rate, $S_{inj.}$ the internal cross-section of the sampling canal and α a coefficient representing the spreading of the injection flow. In the best case (smallest Δx_1) the solute is spread radially over the entire section of the column (S_c) and α is given by

$$\alpha_{lim.} = \frac{S_{inj.}}{S_c} \tag{16}$$

It must be pointed out that the smallest Δx corresponds to the best injection only if we neglect the possible positive effects of operating the column under the conditions of a column of infinite diameter[18,19].

If the injection is very fast, serious turbulences are generated by friction forces between the mobile phase and the incoming jet of sample solution. Eddies can also appear when the syringe is introduced into the injection port and withdrawn. This may result in large values of α.

The injection flow-rate is related to the injection time and volume by

$$F_{inj.} = \frac{V_{inj.}}{t_{inj.}} \tag{17}$$

so that, combining eqns. 14, 15 and 17, we obtain

$$\Delta x_1 = \frac{V_{inj.}}{S_{inj.}(1 + k')\varepsilon_T} \cdot \alpha \tag{18}$$

As far as $u'_{ext.}$ is concerned, we simply have

$$u'_{ext.} = \frac{u_{ext.}}{1 + k'} \cdot \beta \tag{19}$$

where $u_{ext.}$ is the mobile phase velocity around the injection tubing (external velocity) and β a coefficient representing the flow disturbance due to the injection process (deformation of flow lines). It is likely that β depends on the ratio $S_c/S'_{inj.}$ ($S'_{inj.}$ being the external cross-section of the injection canal) and on the injection velocity. *A priori*, β lies between 0 and 1.

The general equation for Δx is therefore

$$\Delta x = \frac{V_{inj.}}{S_{inj.}\varepsilon_T(1 + k')} \cdot \alpha + \frac{u_{ext.}}{1 + k'} \cdot t_{inj.}\beta \tag{20}$$

Noting that $V_0 = LS_c\varepsilon_T$, $t_0 = (L/u)$ and $L = N_{col.}h_{col.}d_p$, we can write

$$\Delta x = \frac{L}{(1+k')}\left[\frac{V_{inj.}}{V_0}\cdot\alpha\frac{S_c}{S_{inj.}} + \frac{t_{inj.}}{t_0}\cdot\beta\cdot\frac{u_{ext.}}{u}\right] \quad (21)$$

Then eqn. 12 becomes

$$h_{out.} = h_{col.} + \frac{N_{col.}h_{col.}}{K^2(1+k')^2}\left[\frac{V_{inj.}}{V_0}\cdot\alpha\cdot\frac{S_c}{S_{inj.}} + \frac{t_{inj.}}{t_0}\cdot\beta\cdot\frac{u_{ext.}}{u}\right]^2 \quad (22)$$

Application to conventional injection methods

We shall now discuss the application of eqns. 20 and 22 to different sampling methods.

Syringe stop-flow injection. In this mode the external mobile phase velocity ($u_{ext.}$) is zero and

$$\Delta x = \Delta x_1 \quad (23)$$

It is difficult to calculate α *a priori*, particularly when the injection is carried out inside a PTFE frit whose permeability is different from that of the column. Eqn. 22 suggests a linear variation of the reduced plate height with $V_{inj.}^2$. However, it will be shown in Part II[8] that such a linearity is not obtained experimentally as the situation is more complex. The typical shape of the h *versus* $V_{inj.}^2$ curves is shown in Fig. 3 and can be explained as follows.

As the injected volume increases from a negligibly small volume, the solute spreads closer and closer to the wall of the column. Provided that the sample volume is small enough to ensure column operation under the conditions of the infinite diameter effect[18,19], $\sigma_{col.}^2$ in eqn. 1 can be considered as constant and $h_{out.}$ increases linearly with $V_{inj.}^2$ as predicted by eqn. 22 (part I of the curve in Fig. 3). When $V_{inj.}$ reaches a particular value ($V_{inj.1}$; *cf.*, Fig. 3), the solute enters the wall region at the end of the column and henceforth h increases more rapidly. The decrease in efficiency is due not only to the increase in $V_{inj.}$ but also to the increase in $\sigma_{col.}^2$. The variation of h with $V_{inj.}^2$ in this range is not necessarily linear. Then $V_{inj.}$ reaches the value $V_{inj.2}$: the sample volume is so large that the sample penetrates the wall region at the inlet of the column. For larger sample volumes, eqn. 18 has to be modified, as now the volume ($V_{inj.} - V_{inj.2}$) is spread over the entire column cross-section and α is $\alpha_{limit.}$. Thus:

$$\Delta x = \frac{V_{inj.2}}{S_{inj.}\varepsilon_T(1+k')}\cdot\alpha + \frac{(V_{inj.} - V_{inj.2})}{S_c\varepsilon_T(1+k')} \quad (24)$$

In fact, as it is likely that there are no sharp boundaries between the various phenomena described, and α depends on $V_{inj.}$, a more rigorous form of eqn. 24 can be written:

$$\Delta x = \left[\frac{1}{S_{inj.}\varepsilon_T(1+k')}\right]\int_0^{V_{inj.}}\alpha\,dV_{inj.} \quad (25)$$

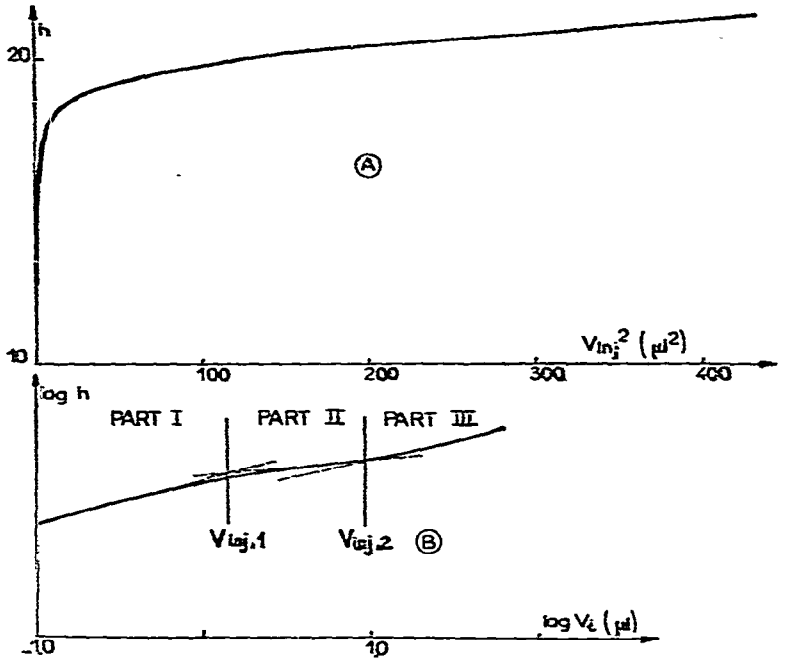

Fig. 3. Theoretical variation of the reduced plate height (h) with the square of the volume ($V_{inj.}^2$).

However, the simpler form (eqn. 24) suggests that the slope of the third part of the h *versus* $V_{inj.}^2$ plot is smaller than that of the first part (*cf.*, Fig. 3), in agreement with experimental results[8].

The values of $V_{inj.1}$ and $V_{inj.2}$ depend on the column and injector geometries and are difficult to predict.

On-line syringe injection. Because the external velocity is different from zero, it is now necessary to take into account the second term, Δx_2. It is worth noting that Δx_2 can be of the same order of magnitude as Δx_1. Assume, for instance, an injection of 5 μl in 0.5 sec in a column of 4 mm I.D., with a total porosity of 0.8. If the internal diameter of the syringe needle is 0.25 mm, then Δx_1 is at least about $0.5/(1 + k')$ mm. When the external flow-rate (which is here the flow-rate in the column) is 1 ml/min, Δx_2 is at most $0.8/(1 + k')$ mm. In most instances, however, Δx_1 will be larger than $0.5/(1 + k')$ and Δx_2 smaller than $0.8/(1 + k')$, but nevertheless Δx_2 cannot be neglected.

On the other hand, the external flow interacts with the sample solution flow inside the injection port and this usually decreases the solute radial diffusion: α for on-line injection will be larger than for stop-flow injection. Experimentally[8], we obtain similar efficiencies with the two injection modes for sample volumes of 2–5 μl.

The phenomenon reported previously for the shape of the h *versus* $V_{inj.}^2$ curve and illustrated in Fig. 3 also occurs in this mode of sampling.

Normal sampling valve. This technique is similar to stop-flow injection but with an important difference. Because the mobile phase enters the column through the sampling canal, there is a permanent radial dispersion of the flow lines at the column inlet. This results in two effects: the solute can readily reach the wall region,

and there are flow lines with very small axial velocity at the column inlet if there is an abrupt change in cross-section[20].

Consequently, although Δx is not markedly larger than for stop-flow injection, $\sigma^2_{col.}$ may be much larger. Moreover, because some solute molecules reach the column top along the wall with a small axial velocity, the peak profile may be unsymmetrical[20] if the wall region is large.

Split sampling valve. The splitting ratio (r) is the fraction of the total flow (F) which goes through the valve. We then have the following relationships:

$$t_{inj.} = \frac{V_{inj.}}{rF}; \; u'_{inj.} = \frac{rF}{S_{inj.}\varepsilon_T(1+k')}; \; u_{ext.} = \frac{(1-r)F}{(S_c - S'_{inj.})\varepsilon_T(1+k')} \tag{26}$$

Eqn. 20 can therefore be written as

$$\Delta x = \frac{V_{inj.}}{S_{inj.}\varepsilon_T(1+k')} \cdot \left[\alpha + \frac{1-r}{r} \cdot \frac{S_{inj.}}{S_c - S'_{inj.}} \cdot \beta\right] \tag{27}$$

The important difference with on-line injection is that the time of injection is no longer an independent variable, but depends on r. The parameters α and β are undoubtly related to r.

For a particular value of r (r_0), the injection velocity is equal to the external velocity. This is isokinetic sampling, which is sometimes considered as ideal. It is easy to show that r_0 is given by

$$r_0 = \frac{1}{1 + \dfrac{S_c - S'_{inj.}}{S_{inj.}}} \tag{28}$$

Finally, we have summarized in Table I the expressions for $u_{ext.}/u$ and Δh.

Influence of injection time and injection volume on column efficiency

In the more general case, eqn. 22 shows that both $V_{inj.}$ and $t_{inj.}$ determine Δh. However, as suggested by Table I, $t_{inj.}$ has no effect in the case of stop-flow and valve injections. We shall therefore examine first the effect of injection volume on column efficiency for these two sampling techniques.

The calculations are made for stop-flow and normal valve injection. With a split valve, it is necessary to introduce the correction term $(\alpha + (1-r)\cdot\beta\cdot S_{inj.}/r(S_c - S_{inj.}))^2$ as shown in eqn. 29.

Effect of injection volume. Eqn. 22 shows that the influence of the injection volume on the h *versus* ν curve (where ν is the solvent reduced velocity) is a constant term, Δh, given by:

$$\Delta h = \frac{V^2_{inj.}}{V^2_R} \cdot \frac{L}{d_p K^2} \left(\frac{\alpha}{\alpha_{lim.}}\right)^2 \tag{29}$$

Eqn. 29 suggests that the effect of injection volume is inversely proportional to the particle size. This statement is valid, however, only if all of the other parameters

TABLE I

$\frac{u_{ext.}}{u}$ AND Δh EXPRESSIONS FOR THE VARIOUS INJECTION SYSTEMS

$S_{inj.}$ and $S'_{inj.}$ are the injection tube internal and external cross-sectional area, respectively. S_c is the column cross-sectional area. r is the splitting ratio, that is, the part of the total flow-rate flowing through the valve.

Injection	$\frac{u_{ext.}}{u}$	Δh
Syringe, stop-flow	0	$\frac{N_{col.}h_{col.}}{K^2(1+k')^2}\left(\frac{V_{inj.}}{V_0}\right)^2\alpha^2\left(\frac{S_c}{S_{inj.}}\right)^2$
Syringe, on-line	$\frac{S_c}{S_c - S'_{inj.}} \approx 1$	$\frac{N_{col.}h_{col.}}{K^2(1+k')^2}\left(\frac{V_{inj.}}{V_0}\cdot\alpha\cdot\frac{S_c}{S_{inj.}}+\frac{t_{inj.}}{t_0}\cdot\beta\cdot\frac{S_c}{S_c-S'_{inj.}}\right)^2$
Normal valve	0	$\frac{N_{col.}h_{col.}}{K^2(1+k')^2}\left(\frac{V_{inj.}}{V_0}\right)^2\alpha^2\left(\frac{S_c}{S_{inj.}}\right)^2$
Split valve	$(1-r)\cdot\frac{S_c}{S_c - S'_{inj.}}$	$\frac{N_{col.}h_{col.}}{K^2(1+k')^2}\left(\frac{V_{inj.}}{V_0}\right)^2\left(\frac{S_c}{S_{inj.}}\right)^2\times\left(\alpha+\frac{1-r}{r}\cdot\beta\cdot\frac{S_{inj.}}{S_c-S'_{inj.}}\right)^2$

in eqn. 29 remain constant. Assume, for instance, that we want to generate a given number of theoretical plates in a given time. Obviously, various column configurations can solve this problem. The mobile phase reduced velocity, ν, is usually calculated by solving the equation

$$h(\nu) = \frac{\nu t_R D_m}{(1+k')Nd_p^2} \tag{30}$$

derived from the classical definition of analysis time, $t_R = L/u\,(1+k')$, by replacing L and u by the reduced plate height and velocity, respectively. $h(\nu)$ is the equation of the reduced plate height curve which characterizes only the contribution of the column to band broadening. The corresponding plate height is $h_{col.}$. It is more relevant to consider the relative contribution of the injection volume to the plate height:

$$\frac{\Delta h}{h_{col.}} = \frac{V_{inj.}^2}{S_c^2\varepsilon_T^2(1+k')^2N_{col.}d_p^2h_{col.}^2K^2}\cdot\left(\frac{\alpha}{\alpha_{lim.}}\right)^2 \tag{31}$$

The variation of $(h_{col.}d_p)^{-2}$ with d_p is shown in Fig. 4. The calculations are made for various capacity ratios, assuming an efficiency of 5000 plates, an analysis time of 5 min and a solute diffusion coefficient of $2\cdot10^{-5}$ cm^2 sec^{-1}. It can be seen from Fig. 4 that within the range of particle size studied, $\log(h_{col.}d_p)^{-2}$ decreases almost linearly with increasing particle size. The larger k', the stronger the dependence of $(h_{col.}d_p)^{-2}$ (and consequently of $\Delta h/h_{col.}$) on d_p. It is noteworthy that increasing the particle size from 5 to 10 μm has the same effect as an increase from 25 to 30 μm.

It is possible to calculate, using eqn. 31, the characteristics of the columns

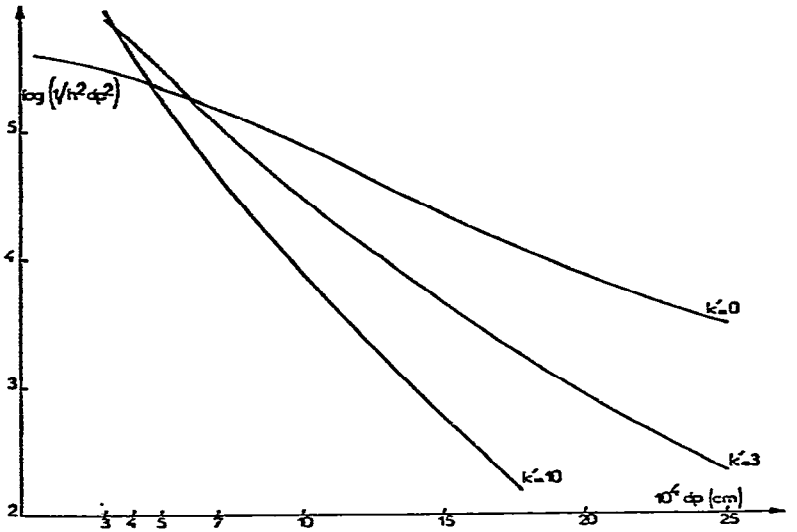

Fig. 4. Variation of $\log (1/h^2 d_p^2)$ with particle size (d_p, μm) for different capacity ratios (k') in order to obtain 5000 theoretical plates in 300 sec. The equation of the reduced plate height curve (see text) is $h = 2/\nu + 2\nu^{0.33} + 2 \cdot 10^{-2}\,\nu$.

such that the relative injection volume contribution is the same, whatever the particle size, all of these columns generating 5000 plates in 5 min. The results are given in Fig. 5. We chose 4.6 mm as the reference for the calculations of the column internal diameter for the column packed with 5-μm particles and $\alpha/\alpha_{\text{lim.}} = 1$. Fig. 5 shows

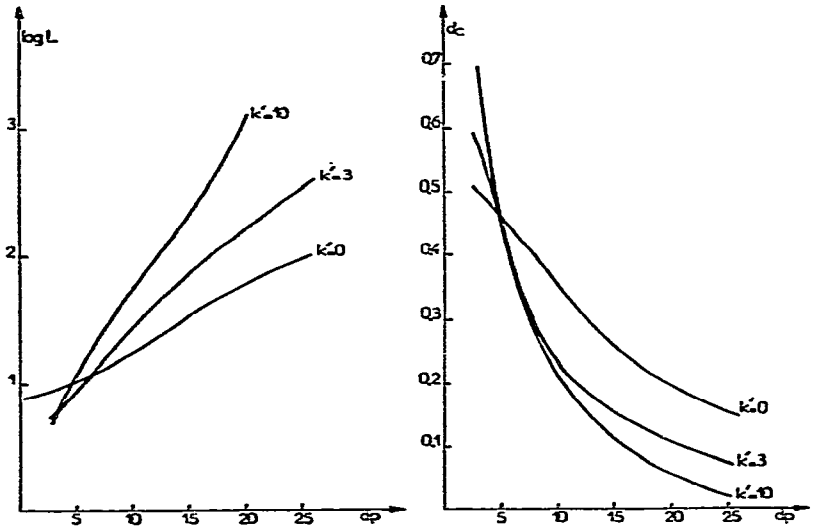

Fig. 5. Variation of the column length (L, cm) and internal diameter (d_c, cm) with the particle size (d_p, μm) for a column yielding 5000 theoretical plates in 300 sec in order to have the same injection volume contribution. The equation of the reduced plate height curve (see text) is $h = 2/\nu + 2\nu^{0.33} + 2 \cdot 10^{-2}\,\nu$.

that for an unretained solute under normalization conditions of efficiency and analysis time, a 10 cm × 4.6 mm I.D. column packed with 5-μm particles is equivalent to an 18 cm × 3.55 mm I.D. column packed with 10-μm particles. Note that assuming $\Delta h/h_{col.}$ and efficiency are constant is equivalent to assuming that the retention volume is constant.

The situation is different when working at constant plate number and maximal column efficiency. This means working at the minimal ($h_{min.}$, $\nu_{opt.}$) of the (h, ν) curve. Under these conditions, eqn. 31 applies with $h_{col.} = h_{min.}$. Eqn. 31 indicates that if the column cross-sectional area is kept constant, the relative injection contribution decreases with d_p^{-2}. It must be kept in mind that under these conditions, the dilution in the column will be greater for the larger particles as the column length is proportional to the particle size. Consequently, in order to keep the same signal-to-noise ratio, it is necessary to inject less on the smaller particle column. Conversely, at constant dilution the injection volume contribution is independent of the particle size.

Effect of injection time. It is possible to control separately $V_{inj.}$ and $t_{inj.}$ only with the syringe on-line injections. If one wants to account all of the advantages of this sampling mode, it is necessary to control carefully the speed of injection. Indeed, too fast injections can give extra band broadening because the solute jet hits the packing and bounces back. On the other hand, too slow injections are not recommended because of the effect of injection time on efficiency. Assuming that the injection volume effect is negligible in comparison with the effect of injection time and that $u_{ext.} = u$, eqn. 22 becomes

$$\Delta h = \frac{t_{inj.}^2 D_m^2 \beta^2}{(1 + k')^2 K^2 L d_p^3} \nu^2 \tag{32}$$

Eqn. 32 indicates that the effect of the injection time is an additional term in the plate height equation. This term is proportional to ν^2. This effect is similar to that of the time constant (τ) of the detector when it is small[4]. Note also that d_p appears to the third power in eqn. 32, which shows a major dependence of this contribution on the particle size.

Assume now that we want to generate a given number of theoretical plates in a given time ($h_{col.}$ is again given by eqn. 30). The relative increase in reduced plate height is given by

$$\frac{\Delta h}{h_{col.}} = \frac{t_{inj.}^2 \beta^2}{K^2 t_R^2} \cdot N_{col.} \tag{33}$$

and now the contribution of injection time is independent of the particle size.

If we are working at constant plate number and maximal column efficiency ($h_{min.}$, $\nu_{opt.}$), the relative increase in reduced plate height is given by the relationship

$$\frac{\Delta h}{h_{min.}} = \frac{t_{inj.}^2 \beta^2 \nu_{opt.}^2 D_m^2}{(1 + k')^2 K^2 N h_{min.}^2 d_p^4} \tag{34}$$

It appears that the effect of injection is divided by 16 when d_p is doubled. This shows

the significant role of the injection time when working with very efficient columns packed with small particles.

CONCLUSION

The effects of sampling on peak width and apparent column performance have been the topic of many discussions and papers. Apparently conflicting experimental results have been reported, and these are reviewed in Part II[8]. The present theory gives a suitable framework for accounting for these complex phenomena. Different injection systems give contributions that do not vary similarly with the experimental conditions, so the best sampling system depends on the problem at hand. The model proposed predicts a non-linear dependence of the plate height on the square of the injection volume, in agreement with experimental results[8]. This effect is more important with columns whose packing is not homogeneous, but are poorly packed against the wall.

The flow pattern at the column inlet and in the very top section of the column is of critical importance[20], and this has long been underestimated. This explains the advantage of syringe injection and split valve injection over the more conventional direct valve injection.

Depending on the conditions under which various columns are compared, the contribution of a given sampling mode may or may not become prohibitive when the particle size is reduced. In any event, sampling is a critical problem in the operation of modern LC columns.

LIST OF SYMBOLS

D_m	Diffusion coefficient of a solute in the mobile phase (eqn. 30).
d_p	Average particle diameter of the stationary phase (eqn. 12).
F	Total column flow-rate (eqn. 26).
$F_{inj.}$	Injection flow-rate (eqn. 15).
H	Height equivalent to a theoretical plate of the column ($L/N_{col.}$, eqn. 8).
h	Reduced height equivalent to a theoretical [illegible] (H/d_p) (eqn. 30).
$h_{col.}$	Column contribution to h (eqn. 12).
$h_{min.}$	Minimum value of h (eqn. 34).
$h_{out.}$	Reduced plate height at column outlet (eqn. 12).
Δh	Contribution of injection process to the reduced plate height (eqn. 12).
K	Constant describing the quality of the injection (eqn. 4).
K^0	Column permeability.
k'	Column capacity factor (eqn. 6).
L	Column length (eqn. 6).
$L_{lim.}$	Characteristic value of L, defined in Fig. 1 and eqn. 8.
$N_{col.}$	Contribution of the column to the number of theoretical plates (eqn. 2).
$N_{inj.}$	Contribution of the injection process to the number of theoretical plates (eqn. 2).
$N_{out.}$	Number of theoretical plates measured at the outlet of the column (eqn. 2).
R_S	Resolution between two peaks.

r	Splitting ratio (eqn. 26).
r_0	Isokinetic value of the splitting ratio (eqn. 28).
S_c	Column cross-section (eqn. 16).
$S_{inj.}$	Internal cross-section of the sampling canal (eqn. 15).
$S'_{inj.}$	External cross-section of the sampling canal (eqn. 26).
$t_{inj.}$	Injection time (eqn. 14).
t_0	Column hold-up time; retention of a non-retained solute (eqn. 21).
t_R	Retention time of a solute (eqn. 2).
Δt_R	Difference between the retention times of two compounds.
u	Flow velocity of the mobile phase in the column (eqn. 6).
$u_{ext.}$	Mobile phase velocity around the syringe needle (eqn. 19).
$u'_{ext.}$	Linear velocity of the zone around the syringe needle (eqn. 14).
$u'_{inj.}$	Linear velocity of the zone corresponding to the injection flow (eqn.14).
v	Velocity of the solute zone (eqns. 5 and 6).
$V_{inj.}$	Injection volume (eqn. 17).
$V_{inj.,1}$ $V_{inj.,2}$	Particular values of the injection volume (Fig. 3).
V_0	Volume of liquid phase inside the column (eqn. 21).
V_R	Retention volume of a solute (eqn. 29).
Δx	Width of the band of solute at column inlet (eqn. 4).
Δx_1	Contribution to injection band width of flow inside the syringe needle (eqn. 13).
Δx_2	Contribution to injection band width of the mobile phase flow (eqn. 13).
α	Coefficient representing the spreading of the injection flow (eqn. 15).
$\alpha_{lim.}$	Limiting value of α (eqn. 16).
β	Coefficient representing the flow disturbance due to the injection process (eqn. 19).
ε_T	Total porosity of the packing (eqn. 15).
ν	Reduced velocity of the mobile phase.
$\nu_{opt.}$	Optimal value of ν.
σ^2	Variance of a peak.
σ_t^2	Variance in time unit (eqn. 1).
σ_x^2	Variance in length unit (eqn. 4).
$\sigma^2_{col.}$	Contribution of the column to the peak variance (eqn. 1).
$\sigma^2_{inj.}$	Contribution of the injection process to the peak variance (eqn. 1).
$\sigma^2_{out.}$	Variance of the peak at column outlet.
τ	Time constant of the detector (Fig. 1).

REFERENCES

1 M. Martin and G. Guiochon, *Chromatographia*, 10 (1977) 194.
2 T. J. N. Webber and E. H. McKerrell, *J. Chromatogr.*, 122 (1976) 243.
3 B. Coq, C. Gonnet and J.-L. Rocca, *J. Chromatogr.*, 106 (1975) 249.
4 H. Colin, A. Jaulmes and G. Guiochon, in preparation.
5 T. W. Smuts, D. J. Solms, F. A. Van Niekerk and V. Pretorius, *J. Chromatogr. Sci.*, 7 (1969) 24.
6 J. J. Kirkland, W. W. Yau, H. J. Stoklosa and C. H. Dilks, Jr., *J. Chromatogr. Sci.*, 15 (1977) 303.

7 C. F. Simpson, in C. F. Simpson (Editor), *Practical High Performance Liquid Chromatography*, Heyden, London, 1977, p. 233.
8 H. Colin, J. C. Diez-Masa, A. Jaulmes and G. Guiochon, in preparation.
9 J. C. Sternberg, *Advan. Chromatogr.*, 2 (1966) 205.
10 R. G. Brownlee and J. W. Higgins, *Chromatographia*, 11 (1978) 567.
11 J. C. Kraak, H. Poppe and F. Smedes, *J. Chromatogr.*, 122 (1976) 147.
12 J. F. K. Huber, J. A. R. J. Hulsman and C. A. M. Meijers, *J. Chromatogr.*, 62 (1971) 79.
13 B. L. Karger, M. Martin and G. Guiochon, *Anal. Chem.*, 46 (1974) 1640.
14 M. Martin, C. Eon and G. Guiochon, *J. Chromatogr.*, 108 (1975) 229.
15 H. Colin and G. Guiochon, *J. Chromatogr.*, 158 (1978) 183.
16 R. P. W. Scott, *J. Chromatogr. Sci.*, 9 (1971) 449.
17 L. R. Snyder, *J. Chromatogr. Sci.*, 10 (1972) 187.
18 J. H. Knox and J. F. Parcher, *Anal. Chem.*, 41 (1969) 1599.
19 J. H. Knox, G. R. Laird and P. A. Raven, *J. Chromatogr.*, 122 (1976) 129.
20 B. Coq, C. Cretier and J. L. Rocca, *Analusis*, 7 (1979) 339.